Supporting Information

Zangmeister et al. 10.1073/pnas.1403768111

SI Methods

Soot Aggregate Packing. Soot was generated using a Santoro-style diffusion burner operating using ethylene fuel. Freshly generated soot particles were allowed to aggregate in a 5-L aging chamber for ∼30 s, forming a lacey fractal morphology. Soot particles were collapsed into a compact spherical morphology through water condensation and subsequent rapid evaporation by passing the soot through a H_2O growth tube consisting of a condenser at 10 °C and a hydrator at 45 °C, followed by drying the particles with a tube furnace at 150 °C between a pair of SiO_2 diffusion dryers. Size and mass selection was conducted by passing soot through a differential mobility analyzer (DMA) and aerosol particle mass analyzer (APM), respectively, and particles were counted using a condensation particle counter (CPC). The use of a tandem DMA-APM-CPC for measuring particle mass as a function of mobility diameter (D_p) is well detailed in ref. 1. Mass distributions were fit using a Gaussian function over the range where only the (+1) charged particle of interest was present (2, 3). The average mass was used to calculate the mass-mobility scaling exponent (D_f). Packing density was calculated from the measured mass assuming the spherical volume was defined by the particle mobility diameter, a valid assumption for particles with $D_f = 3$. Monomer diameter was measured using transmission electron microscopy (TEM) of soot aerosol electrostatically deposited on lacey carbon grids.

Macroscale Aggregate Packing. Monodisperse spherical polymer spheres with a diameter of 0.60 cm and a mass of 0.120 ± 0.002 g were combined to form aggregated particles. Particles examined ranged from one-unit monomers through 12-unit (N) aggregates. Monomer units were adhered together in random rigid 3D conformations using a small amount of solvent. Dimers and trimers were initially constructed and added to form larger aggregates. For $N \geq 3$, $\sim 10^3$ aggregates were prepared, and a typical measurement used 30–50% of the aggregates at each N. Aggregate dimension was characterized by measuring effective density (ρ_{eff}) as a function of N, and show ρ_{eff} is constant at $N \geq 4$ (Fig. S2). Aggregate aspect ratio (aggregate length/width) was measured for $4 \leq N \leq 12$ was 1.88 ± 0.22. Monomer and aggregate packing was measured in cylindrical and spherical chambers of known volume and varying diameters.

Monomer units and assembled aggregates were added to packing chambers and tapped gently to allow the particles to gravitationally settle into the chamber volume. Particle number concentration and subsequent packing density was determined from the mass of particles within the packing chamber and the volume occupied by the particles. The packing densities of the randomly oriented aggregates were measured for each value of N in triplicate by multiple individuals with each measurement representing a random and unique population of aggregates. After each measurement, aggregates were removed from the vessel and a new, unique aggregate population was measured. Data were averaged for each user and each vessel for all values of N and uncertainties pooled.

To ensure that wall effects were not influencing θ_f, we measured θ_f as a function of vessel diameter (D) that spanned several monomer radius (a). Each datum shown in Fig. S3*A* is the average of three measurements at a given D, for D from 1.7 to >16. From the plot, wall effects are easiest to observe for low N. For N=1, where θ_f spans from 0.36 (D = 1.73, a volume with a diameter ∼1.5a and a = 0.6 cm) to the jammed packing limit, $\theta_f \approx$ 0.64 for containers with large diameters, $D > 10$. Data of θ_f as function of D/a for N = 1, 4, 8, and 12, shown in Fig. S3*B*, indicate that wall effects are minimized for $D/a > 6$. The regime where wall interaction limits θ_f (small D/a) are shown using the filled red circles in Fig. S3*A* ($\theta_f \sigma \geq 2$ for $N = 1$). Larger D/a are included in the reported data shown in Fig. 2.

Determination of N_T for Comet 103P/Hartley 2. Comet mass was from ref. 3, showing the mass of Comet 103P/Hartley 2 as 1% of comet Tempel 1, or 5.15×10^{14} g. We used 100-nm dust grains from ref. 4, assumed sphericity and a density (ρ) of 3.4 g/cm^3, as listed in ref. 5 for Tempel 1 dust grains. Grains had a mass of 1.8×10^{-18} kg per monomer. Assuming $N = 10$, the nucleus is composed of 3×10^{28} aggregates (N_T).

For aggregated systems, R_g scales linearly with N, as shown in Fig. S4.

1. Ma X, Zangmeister CD, Gigault J, Mulholland GW, Zachariah MR (2013) Soot aggregate restructuring during water processing. *J Aerosol Sci* 66:209–219.
2. Radney JG, et al. (2013) Direct measurements of mass-specific optical cross sections of single-component aerosol mixtures. *Anal Chem* 85(17):8319–8325.
3. Ma X, Zangmeister CD, Gigault J, Mulholland GW, Zachariah MR (2013) Soot aggregate restructuring during water processing. *J Aerosol Sci* 66(0):209–219.
3. Lisse CM, et al. (2009) Spitzer Space Telescope observations of the nucleus of Comet 103P/Hartley 2. *Publ Astron Soc Pac* 121(883):968–975.
4. Thomas PC, et al. (2013) Shape, density, and geology of the nucleus of Comet 103P/Hartley 2. *Icarus* 222(2):550–558.
5. Kelley MS, et al. (2013) A distribution of large particles in the coma of Comet 103P/Hartley 2. *Icarus* 222(2):634–652.

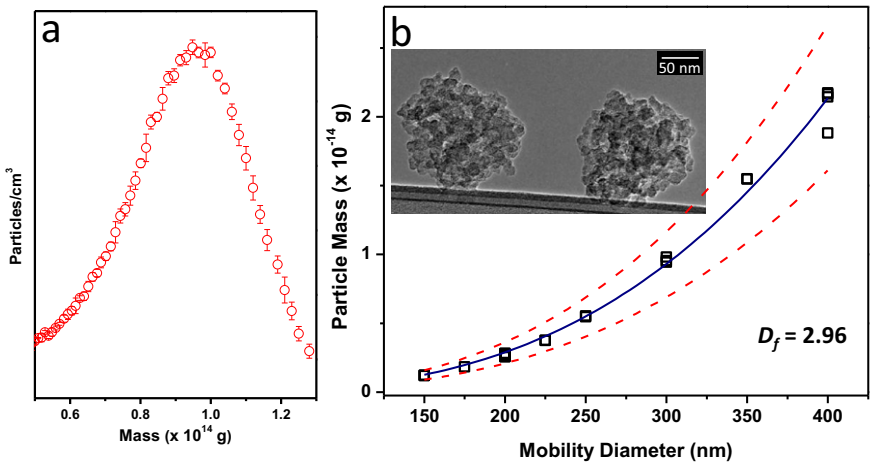

Fig. S1. (*A*) Mass distribution of 300-nm mobility diameter compact soot particles. (*B*) Measured mass of compact soot as a function of mobility diameter. Squares are data from individual experiments. Line represents power-law fit to data with $D_f = 2.96$. Dashed lines are FWHM of mass distribution. (*Inset*) TEM image of compacted soot.

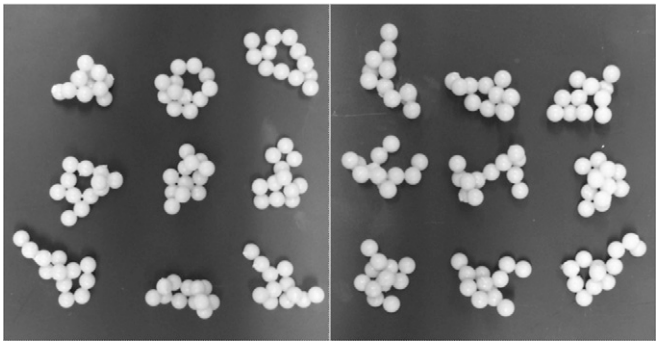

Fig. S2. Aggregates made in random, rigid conformations. Several hundred aggregates were made for each *N*. Representative $N = 12$ aggregates with 0.6-cm monomers are shown.

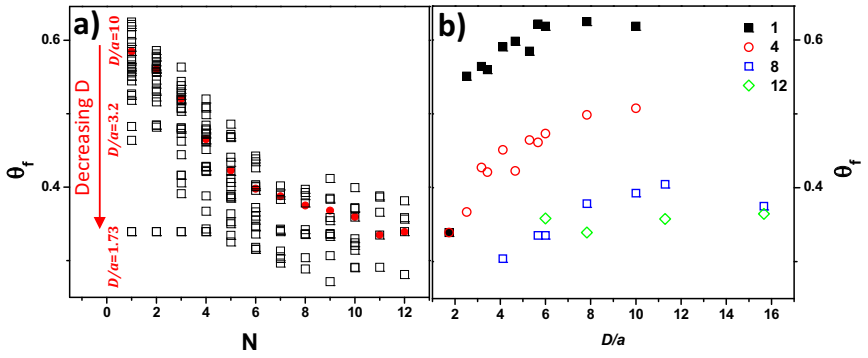

Fig. S3. (*A*) Data ofθ_f as a function of *N* for various vessel cylindrical vessel geometries. Solid circles represent where wall effects impact θ_f. (*B*) Data of θ_f as function of *D*/*a* for $N = 1$ (black squares), 4 (red open circles), 8 (blue open squares), and 12 (green open diamonds) is shown in Fig. S3*B*.

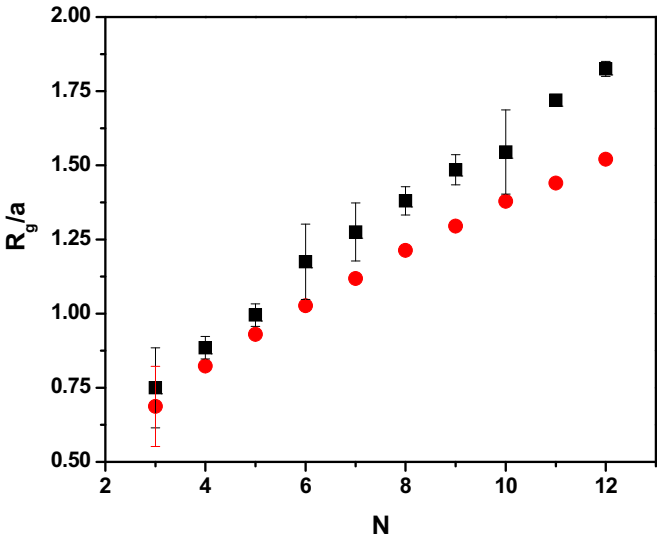

Fig. S4. Dependence of D_f as a function of N for D_f of 1.55 (black squares) and 1.80 (red circles). Error bars represent 1σ.